New satellite climate data records indicate strong coupling between recent frozen season changes and snow cover over high northern latitudes

2015 Environ. Res. Lett. 10 084004

(http://iopscience.iop.org/1748-9326/10/8/084004)

Environmental Research Letters

LETTER

New satellite climate data records indicate strong coupling between recent frozen season changes and snow cover over high northern latitudes

Youngwook Kim[1], **J S Kimball**[1], **D A Robinson**[2] **and C Derksen**[3]

[1] Numerical Terradynamic Simulation Group, College of Forestry and Conservation, The University of Montana, Missoula, MT 59812, USA
[2] Department of Geography, Rutgers University, Piscataway, NJ 08854, USA
[3] Climate Research Division, Environmental Canada, Toronto, ON M3H5T4, Canada

E-mail: youngwook.kim@ntsg.umt.edu

Keywords: freeze thaw, snow cover, remote sensing, frozen ground, snowmelt, NASA MEASURES, soil temperature

Supplementary material for this article is available online

OPEN ACCESS

RECEIVED
17 March 2015

REVISED
22 June 2015

ACCEPTED FOR PUBLICATION
3 July 2015

PUBLISHED
3 August 2015

Abstract

We examined new satellite climate data records documenting frozen (FR) season and snow cover extent (SCE) changes from 1979 to 2011 over all northern vegetated land areas (⩾45 °N). New insight on the spatial and temporal characteristics of seasonal FR ground and snowpack melt changes were revealed by integrating the independent FR and SCE data records. Similar decreasing trends in annual FR and SCE durations coincided with widespread warming (0.4 °C decade^{-1}). Relatively strong declines in FR and SCE durations in spring and summer are partially offset by increasing trends in fall and winter. These contrasting seasonal trends result in relatively weak decreasing trends in annual FR and SCE durations. A dominant SCE retreat response to FR duration decreases was observed, while the sign and strength of this relationship was spatially complex, varying by latitude and regional snow cover, and climate characteristics. The spatial extent of FR conditions exceeds SCE in early spring and is smaller during snowmelt in late spring and early summer, while FR ground in the absence of snow cover is widespread in the fall. The integrated satellite record, for the first time, reveals a general increasing trend in annual snowmelt duration from 1.3 to 3.3 days decade^{-1} ($p < 0.01$), occurring largely in the fall. Annual FR ground durations are declining from 0.8 to 1.3 days decade^{-1}. These changes imply extensive biophysical impacts to regional snow cover, soil and permafrost regimes, surface water and energy budgets, and climate feedbacks, while ongoing satellite microwave missions provide an effective means for regional monitoring.

1. Introduction

The seasonal freeze/thaw (FT) state transition to predominantly non-frozen (FR) conditions in the spring initiates processes that are nearly dormant during the winter FR season and is related to seasonal snowmelt and soil thawing in high northern latitude (HNL) ecosystems (Kimball *et al* 2001, Euskirchen *et al* 2007, Mortin *et al* 2012). The FT signal and associated FR season metric obtained from satellite microwave remote sensing characterizes the predominant FR or non-FR status of the land surface and the duration of FR conditions within the sensor footprint, without distinguishing among individual landscape elements, including vegetation, snow cover and surface soil conditions (Zhang *et al* 2011, Kim *et al* 2012). Snow cover extent (SCE) exerts a strong impact on surface climate and FT conditions by providing an effective thermal buffer reducing soil-atmosphere energy exchange and maintaining warmer winter soil temperatures than would otherwise occur under snow free conditions (Wang and Zender 2011, Mortin *et al* 2012). SCE and FT variations are also coupled with the lower atmosphere by regulating surface energy partitioning of net solar radiation into sensible and latent heat through associated changes in land

surface albedo and evaporation (Betts *et al* 2014). Recent widespread decreasing trends in the FR season and SCE over HNL land areas (⩾45 °N) have been reported (Dye 2002, Brown and Robinson 2011, Derksen and Brown 2012, Kim *et al* 2012) and may be associated with rising atmospheric heating (Dye 2002, Mioduszewski *et al* 2014), and accelerated by an amplified snow-albedo feedback (Chapin *et al* 2005, Dery and Brown 2007).

In a typical HNL seasonal snow cycle, snowmelt may last for several days to weeks in the spring until the snowpack is depleted and nighttime temperatures remain above freezing (Semmens *et al* 2013); surface air temperatures (SATs) may rise above freezing under daily solar radiation and thermal loading, while snow and underlying soil temperatures remain near 0.0 °C or below freezing until the snow cover heat sink is gone. The seasonal transition from dry to wet snowpack conditions with spring snowmelt onset generally coincides with a rapid decline in land surface albedo (Ling and Zhang 2003, Betts *et al* 2014), increased liquid water availability in the landscape (Kimball *et al* 2001, Mortin *et al* 2012) and a seasonal shift in the surface energy budget from predominantly sensible to latent energy, with commensurate increases in land surface evaporation (Chapin *et al* 2005, Ling and Zhang 2003, Zhang *et al* 2011). Prior to the beginning of the HNL snow cycle, FR ground conditions may occur in early to mid-fall before persistent snow cover (Kim *et al* 2014a). FR conditions without a buffering snow layer may promote colder soil temperature extremes, damaging vegetation and reducing subsequent winter soil decomposition and respiration processes (Daniels *et al* 2011, Kreyling *et al* 2012, Aanderud *et al* 2013, Du *et al* 2013). Differences in the seasonal timing and extent of FT and snow cover may also impact other ecosystem properties, including soil active layer development, permafrost temperature and soil organic carbon content (Haei *et al* 2013, Ling and Zhang 2003, Park *et al* 2014).

Despite significant impacts of snow cover status on the terrestrial energy budget and associated carbon and climate feedbacks, few studies have examined regional changes in snow cover conditions over the HNL domain other than documenting changes in SCE. In this study, we document relationships between FR season and SCE changes over the HNL domain (i.e., vegetated land area poleward of 45 °N) using new satellite climate data records (CDRs) for these parameters extending over more than 30 years (1979–2011). We characterize seasonal offsets between FR area and SCE, and regional trends and temporal correlations in these parameters. Finally, we quantify emergent regional patterns and trends in the snowmelt season and FR ground duration over snow-free land areas by integrating the satellite microwave FT and the combined visible-band and microwave sensor based SCE data records.

2. Data and methods

2.1. Satellite data

Satellite passive microwave remote sensing is well-suited for FT monitoring over the HNL domain due to strong contrast in land surface dielectric properties and brightness temperature (T_b) between predominantly FR and non-FR conditions, enhanced by the relative insensitivity of lower frequency (e.g. ⩽ 37 GHz) microwave retrievals to solar illumination and atmosphere cloud/aerosol contamination constraints (Kim *et al* 2011, Frei *et al* 2012). We used a global landscape FT Earth system data record (FT-ESDR) derived from calibrated 37 GHz, vertically polarized and overlapping T_b records from the scanning multi-channel microwave radiometer and special sensor microwave imager; the FT-ESDR distinguishes twice daily (AM and PM) FT conditions from ascending and descending orbit T_b retrievals, posted to a 25 km resolution EASE-Grid (Brodzik and Knowles 2002) for the period 1979–2012 (Kim *et al* 2012, 2014b). Four categorical daily FT classifications are distinguished, including FR (AM and PM FR), non-FR (AM and PM thawed), transitional (AM FR and PM thawed) and inverse transitional (AM thawed and PM FR) conditions. The reported mean annual FT-ESDR spatial classification accuracy exceeds 84% over the HNL domain, but with approximately 7% lower accuracy during seasonal FT transition periods in spring and fall (Kim *et al* 2012). The FT retrieval represents predominant FR or non-FR conditions within the satellite footprint and does not distinguish individual landscape elements, including air, soil, vegetation and snow cover within each 25 km resolution grid cell (Zhang *et al* 2011, Kim *et al* 2012).

FR duration was defined from the daily FT record of the number of FR or transitional days for annual and seasonal periods (table S1). The four seasons are defined as Winter (December–February), Spring (March–May), Summer (June–August) and Fall (September–November), because seasonal snow melt and onset generally occur during spring and fall portions of the calendar year, respectively (Robinson and Frei 2000, Dye 2002).

The HNL FR duration temporal trend patterns were compared against daily 2 m SAT estimates from the quarter-degree resolution ERA-Interim global reanalysis (Dee *et al* 2011). Satellite global CDRs of weekly SCE (Brodzik and Armstrong, 2013) projected in a consistent 25 km resolution EASE-Grid format (Brodzik *et al* 2012) were used to examine seasonal SCE trends and correlations with HNL FR duration changes for the 1979–2011 period. The SCE observations were regridded from the NOAA snow chart CDR (Brown and Robinson 2011, Estilow *et al* 2013) which spans 1967–present (http://snowcover.org), and is manually derived by analysts from combined visible-band satellite imagery, including advanced very high resolution radiometer, geostationary operational

environmental satellite and moderate resolution imaging spectroradiometer records (Helfrich *et al* 2007). Analysis of the updated SCE record indicates improved data quality during the Northern Hemisphere spring (Brown and Robinson 2011). For this study we selected the period 1979–2011, because the FT-ESDR was available from 1979 to 2012 and the SCE data records only extended up to 2011 at the time of this investigation. We examined seasonal and annual SCE duration, defined as the percentage of time in a given period that each grid cell was snow covered, ranging from 0 to 100 percent (table S1). SCE duration is preferred over the binary classification because it can more accurately account for SCE variability in patchy snow areas (Nolin 2010).

The satellite FT and SCE records were integrated to estimate the extent and duration of snowmelt and FR ground conditions. Snowmelt was defined for grid cells where the SCE record indicated snow cover presence, but the FT-ESDR indicated transitional (AM FR, PM non-FR) FT conditions. FR ground cells were defined for coincident FT-ESDR defined FR and snow-free SCE conditions. Durations of snowmelt and FR ground were defined from the weekly data record of the number of grid cells for annual and seasonal periods (table S1). Weekly FT status was determined for each grid cell from the daily FT-ESDR using a 50% temporal threshold within the corresponding coarser 7-day SCE time step. The resulting snowmelt and FR ground metrics were then aggregated on a similar seasonal and annual basis as the FR and SCE metrics described above. The combination of SCE and FT transitional conditions was used as a more conservative indicator of snowmelt relative to the potential addition of FT-ESDR defined non-FR (AM and PM non-FR) conditions. This was done to minimize potential impacts from assumed greater SCE retrieval uncertainty under patchy and transient snow cover conditions later in the spring melt season when non-FR (AM and PM) conditions are more prevalent (Brown *et al* 2007, Kim *et al* 2014a). Here, FT-ESDR classified transitional conditions coinciding with SCE defined snow cover are assumed to represent snowmelt and associated wet snowpack conditions. Likewise, the use of only FT-ESDR defined FR (AM and PM FR) status to estimate FR ground conditions represents a more conservative indicator than the potential use of both FR and transitional (AM FR PM non-FR) FT states.

2.2. Statistical methods

Annual trends were calculated using pre-whitened Kendall's tau statistics following removal of temporal autocorrelation using the ZYP package in *R* statistics (Yue and Pilon 2004). When trends were analyzed, outliers were screened as a non-systematic variation identified on a grid cell-wise basis as quantities surpassing ±2 times the standard deviation (SD) of the long-term record means to minimize any remaining sensor discontinuity occurring from inter-sensor calibration and resolution difference of various satellite sensors (Jeganathan *et al* 2014, Kim *et al* 2014b).

The Spearman's correlation coefficient (*r*-value) was used to assess the sign and strength of relationships between FR and SCE duration anomalies on an annual and seasonal basis. Temporal anomalies of the parameter series were initially computed as annual differences from average conditions characterized from the period of record; where a significant ($p \leqslant 0.1$) trend was identified, the temporal anomalies were determined as differences from the long-term detrended mean (Barichivich *et al* 2014, Kim *et al* 2014c). The significance of these relationships was stratified according to relative strong ($p \leqslant 0.05$), moderate ($0.05 < p \leqslant 0.1$) and weak ($p > 0.1$) categories. The correlations between annual FR and SCE duration anomalies were determined for each grid cell within the HNL domain and analyzed within different segmentation levels determined from independent ancillary geospatial data, including latitudinal zones, characteristic seasonal snow types determined from a 0.45-degree resolution snow physical properties database (Sturm *et al* 1995), and 0.1-degree resolution Köppen climate zone map (Peel *et al* 2007). For consistency, all data records used in this investigation were resampled to the same 25 km resolution EASE-grid format using nearest-neighbor resampling of coarser resolution grid cells or drop-in-bucket averaging of finer resolution pixels. The HNL domain in this study includes all vegetated land areas where seasonal FR temperatures are a major constraint to land surface water mobility and ecological processes over the area poleward of 45 °N, while approximately 63% of the HNL domain is also underlain by permafrost (Brown *et al* 2014).

3. Results

3.1. Correspondence between FR season and snow cover variability

The satellite records show similar trends (1979–2011) in FR and SCE durations over the HNL domain (table 1), with strong declines in FR and SCE durations for the spring and summer. Strong decreasing regional trends in FR and SCE durations occur in summer over both Eurasia (EA) and North America (NA), but with relatively stronger decline over NA. The decreasing trend in mean annual FR duration over the HNL is largely driven by strong decreasing spring and summer FR trends, offset by moderately increasing fall and strongly increasing winter FR trends. A stronger decreasing mean annual FR season trend over EA results from a strong FR duration decrease in spring relative to NA. The mechanisms for fall and winter cooling are uncertain, but coincide with reported snow cover increase (Bulygina *et al* 2009) and fall/winter

Table 1. Kendall's tau trends for mean annual and seasonal frozen (FR) duration (days decade^{-1}) and seasonal SCE duration (% decade^{-1}) enclosed in parentheses for HNL and continental North America (NA) and Eurasia (EA) sub-regions, and 1979–2011 record; trend significance levels are denoted by asterisks as: *moderate ($0.05 < p \leqslant 0.1$) and **strong ($p \leqslant 0.05$).

	Annual	Winter	Spring	Summer	Fall
HNL	−0.49 (−0.21)	0.38* (0.35)	−1.96** (−1.48)	−0.44** (−0.69**)	1.30 (0.85)
NA	−0.59 (−0.07)	0.31 (0.60**)	−0.85 (0.66)	−0.53** (−0.97*)	1.39 (0.20)
EA	−1.39* (−0.03)	0.48* (0.18)	−2.29** (−1.47)	−0.39** (−0.74**)	1.21 (1.56*)

cooling attributed to summer warming and sea ice decline (Cohen *et al* 2012a, 2012b). Relatively weak or inconsistent seasonal SCE trends may result from potential SCE overestimation during spring and fall over some northern land areas (Brown *et al* 2007, Brown and Derksen 2013, Mudryk *et al* 2014), likely due to remaining cloud contamination in the satellite visible band sensor data (Tang *et al* 2013). The mean annual FR season changes also correspond with ERA-Interim SAT annual anomalies over the HNL (correlation (r) = −0.297; $p < 0.1$), NA ($r = -0.503$; $p < 0.05$) and EA ($r = -0.563$; $p < 0.05$). Mean annual and seasonal correlations between FR and SCE duration anomalies over the HNL and NA, and EA portions of the domain are summarized in table 2. FR season variability generally coincides with similar annual and seasonal changes in SCE duration. A relatively weak HNL correlation in spring contrasts with stronger correspondence for continental sub-regions and may reflect opposing oscillations in spring climate conditions between EA and NA (Zhang *et al* 2007). The HNL correlations between annual FR season and SCE variations (figure 1) are predominantly positive, indicating a general SCE retreat coincident to FR duration decreases. The sign and strength of the mean correlations vary according to latitude, with generally stronger, positive correspondence at higher latitudes (figure 2(a)); the correlations are also lower or negative where the FR and SCE seasons occur over a smaller portion of the annual cycle, and consistent with the generally shorter cold season at lower latitudes. The correlations of FR and SCE durations also vary according to regional climate and characteristic snow cover conditions. Lower correlations occur in maritime, prairie and alpine snow conditions, whereas relatively higher correlations occur in tundra and taiga snow zones (figure 2(b)). Alpine and maritime snow areas are characterized by complex terrain and microclimate heterogeneity that may not be effectively resolved by the coarse (25 km) resolution satellite retrievals (Du *et al* 2014). Maritime and prairie snow areas are also characterized by ephemeral or shallow, patchy snow conditions and lower SCE duration (Painter *et al* 2009, Betts *et al* 2014) that may vary independent of FR season changes. Negative correlation areas also coincide with lower latitude temperate and dry climate zones, including Central NA and Western Europe (figure 1). In these areas, longer FR durations coincide with colder, drier atmosphere conditions that promote less precipitation and snow cover. In lower latitude dry climate areas, significant snow cover may also be lost to the atmosphere through wind redistribution and sublimation even under FR temperatures (Bewley *et al* 2010, Callaghan *et al* 2011), while both conditions can result in negative correlations of FR and SCE durations.

Table 2. Spearman's correlations between mean annual and seasonal FR duration (days) and SCE duration (%) anomalies for the NHL domain and continental sub-regions of North America (NA) and Eurasia (EA) over the 1979–2011 record; significance levels denoted by asterisks as *moderate ($0.05 < p \leqslant 0.1$) and **strong ($p \leqslant 0.05$).

	Annual	Winter	Spring	Summer	Fall
HNL	0.399**	0.502**	0.133	0.359**	0.351**
NA	0.493**	0.501**	0.667**	0.215	0.546**
EA	0.527**	0.501**	0.470**	0.481**	0.346**

3.2. Snowmelt and FR ground characteristics

The climatology of HNL FR area and SCE variations established from the long-term satellite records reveals a large dynamic seasonal range and strong interannual variability in the temporal progressions of these parameters (figure 3). The HNL FR area ranges from a summer minimum of approximately 0.2 million km^2 (temporal SD ±0.97 million km^2 mo^{-1}) to a winter maximum of 32.5 million km^2 (SD ± 0.60 million km^2 mo^{-1}). The mean differences between FR area and SCE are approximately 1.0 and 2.7 million km^2 (3.0% and 8.1% of the domain) for respective seasonal transition periods in spring and fall. FR area generally exceeds SCE in the fall and spring, confirming that FR conditions are a prerequisite for persistent fall and winter snow cover, whereas SCE exceeds FR conditions during wet snow conditions in mid-spring and early summer.

Prevailing FR or SCE grid cells are defined in figure S1, where classified FR or snow covered conditions exceed 50% of respective spring and fall periods over the entire record (1979–2011). FR areas generally exceed SCE in the early spring, while SCE exceeds FR area where snowmelt is occurring in the late spring and early summer, extending from generally coastal and southern areas in early spring to inland areas and northern latitudes as the melt season progresses. In the fall, FR areas occur in the absence of snow cover over large areas including portions of Asia and the Pacific Northwest.

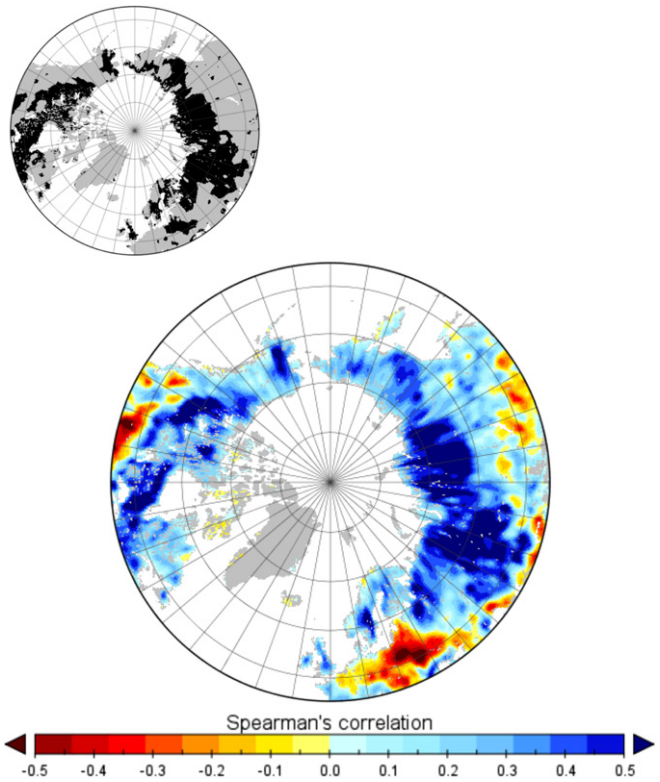

Figure 1. Pixel-wise Spearman correlations (r) between annual FR season (days) and snow cover extent (SCE) duration (%) anomalies for the 1979–2011 record; areas outside the HNL domain are denoted in grey (land) and white (100% open water). Black areas on adjacent inset map represent significant ($p < 0.1$) correlations. Spatial convolution of a Gaussian weighting filter was applied to these maps.

The estimated mean annual number of weeks of respective snowmelt and FR ground durations derived from the integrated FT and SCE records are 3.8 ± 1.7 (spatial-SD) weeks and 0.6 ± 1.1 (spatial-SD) weeks for the 33-year record and the HNL domain (figure 4). The highest mean snowmelt durations are located along the western NA coastal mountain zone, including Southern Alaska, coastal British Columbia, CN and the Pacific Northwest, USA (figure 4(a)). These regions are characterized by cool to moderate climate conditions with extensive orographic driven precipitation and seasonal snow cover, increasing in depth and duration at higher elevations (Daly *et al* 2008). Moderate winter temperatures, humid atmosphere conditions, and frequent rain-on-snow events in this region promote frequent thawing and re-freezing of the snowpack, and transient snow cover conditions at lower elevations that contribute to the extended snowmelt season (Callaghan *et al* 2011). The snowmelt duration is generally shorter in colder and drier climate areas, including boreal and Arctic zones characterized by stable winter FR temperatures and relatively rapid seasonal snowmelt onset, and snow cover depletion (Sturm *et al* 1995, Pomeroy *et al* 2006). In addition to climate constraints, snowmelt duration is also related to snow depth and vegetation stature (Sturm *et al* 2005, Marsh *et al* 2010). Longer FR ground durations coincide with lower latitude temperate and dry climate zones, including central NA, large portions of Europe and Southeastern EA (figure 4(b)). FR ground conditions in the absence of insulating snow cover is less frequent for colder and higher latitude boreal and Arctic domains, where the FR season and SCE records are more tightly coupled (e.g., figure 2(a)).

The Kendall's tau regional trends for snowmelt and FR ground duration determined from the integrated FT and SCE records are presented in figure 5. These results show significant HNL regional trends of decreasing FR ground duration ($p < 0.01$) and increasing snowmelt duration ($p < 0.01$) over the 33-year record. The HNL mean annual snowmelt duration is increasing by approximately 0.19 weeks decade^{-1} while the FR ground duration is decreasing by −0.18 weeks decade^{-1} (figure 5(c)). These trends also coincide with a 0.44 °C decade^{-1} ($p < 0.05$) HNL warming trend derived from the ERA-interim SAT record. The relatively strong regional trends in snowmelt and FR ground durations from the integrated satellite record contrast with relatively weak or inconsistent SCE trends (table 1), and are largely driven by regional warming and associated increasing trends in the frequency of transitional FT events, and longer non-FR seasons (Kim *et al* 2014a). However, the increase in annual wet snowpack duration predominantly reflects increasing snowmelt duration in the fall (0.17 weeks

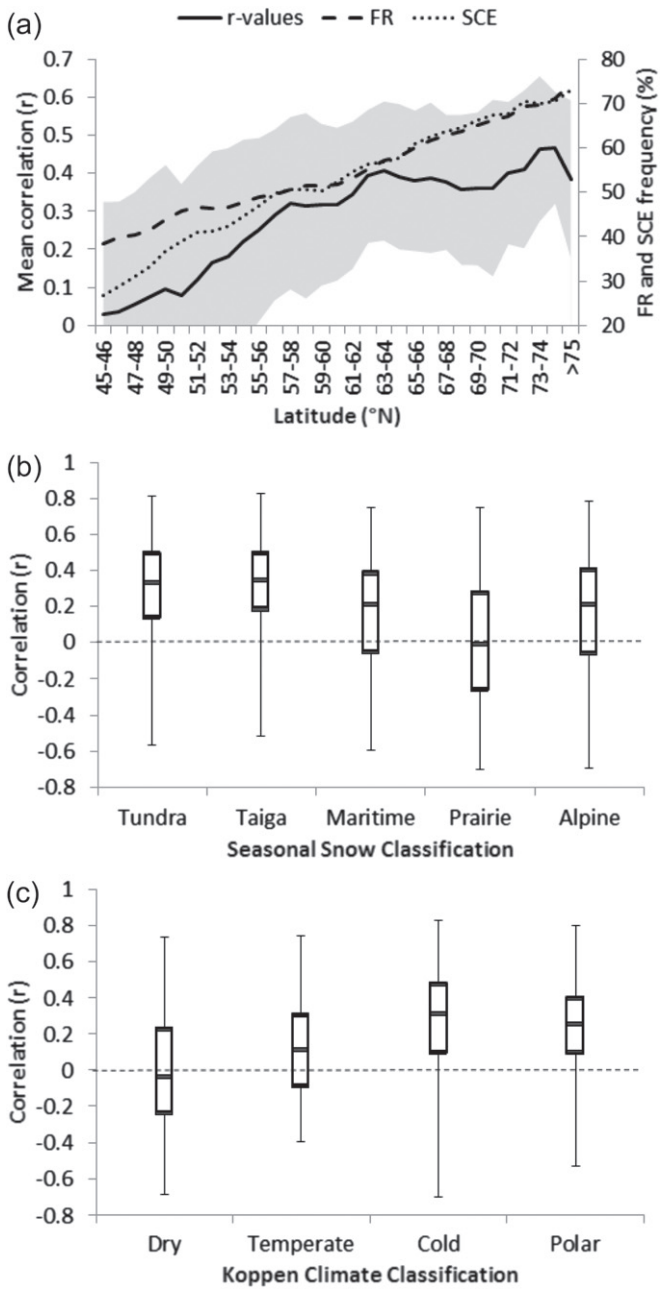

Figure 2. Mean correlation (r) values between HNL FR and SCE duration anomalies binned by (a) latitude, (b) characteristic seasonal snow type and (c) Köppen climate classification defined from independent ancillary geospatial data. The FR and SCE frequencies are defined as the proportion (%) of the annual cycle (365 days) that each grid cell was frozen and snow covered, respectively, and averaged for the period 1979–2011. Gray shading (a) and error bars (b), (c) denote one spatial standard deviation around the means.

decade^{-1}; $p < 0.05$) rather than the other seasons (table S2); this implies more frequent occurrence of transient snow cover and snowmelt prior to the onset of a more persistent seasonal snowpack in the fall, while the decrease in FR ground conditions is more uniformly distributed throughout the annual cycle (table S2).

The trend pattern of snowmelt and FR ground durations is spatially complex (figure 5). The snowmelt duration trend map shows a general lengthening of the snowmelt season over western NA and eastern EA. Significant ($p < 0.1$) increasing and decreasing trends in snowmelt duration represent approximately 22.0% and 4.4% of the HNL domain, respectively. The significant positive snowmelt duration trend areas average 0.76 ± 0.29 (spatial SD) weeks decade^{-1} (figure 5(a)) and are four times larger than the HNL regional trend (figure 5(c)). Widespread increases in snowmelt duration may reflect increasing winter snow accumulations (table 1) and more frequent transitional FT conditions associated with regional warming trends (Bulygina *et al* 2009, Kim *et al* 2012). Significant increasing and decreasing trends in annual FR ground duration represent approximately 0.7% and 4.9% of the domain, respectively (figure 5(b)); the significant negative trend areas show a mean FR ground duration

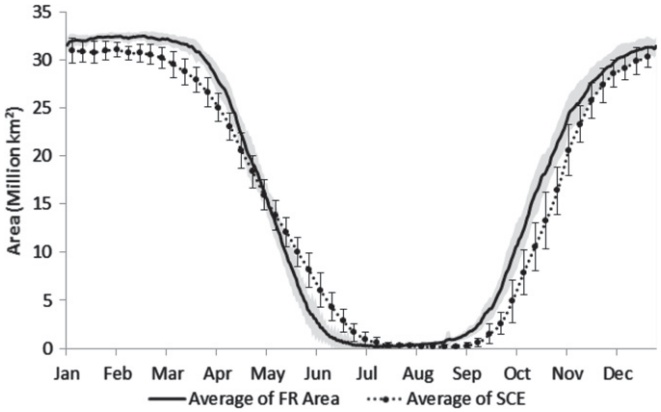

Figure 3. Mean daily climatology of frozen (FR) area and weekly snow cover extent (SCE) over the 1979–2011 record and HNL domain; gray shading and error bars denote one temporal standard deviation around the regional means, determined from the satellite data records.

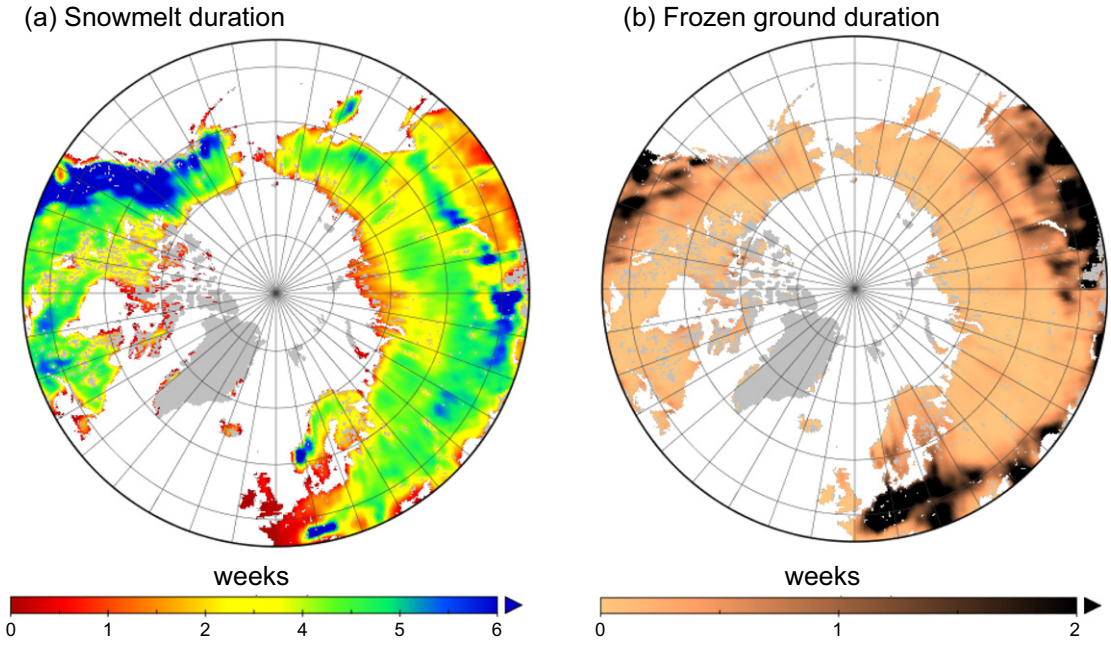

Figure 4. Mean annual snowmelt (a) and frozen ground (b) duration (weeks) over the 1979–2011 record and HNL domain; areas outside the domain are denoted in grey (land) and white (100% open water). Spatial convolution of a Gaussian weighting filter was applied to these maps.

decrease of -0.75 ± 0.38 (spatial SD) weeks decade^{-1}, which is 4.2 times larger than the HNL regional trend (figure 5(c)). Widespread decreasing FR ground duration trends are predominantly located along the southern HNL domain, while northern boreal and Arctic areas show generally weak, increasing trends.

4. Discussion

In this study, we utilized recent global satellite CDRs to analyze FR season and SCE changes over the HNL domain from 1979–2011, and provided new insight on seasonal snowmelt and FR ground changes revealed by a novel data fusion approach integrating the two independent and relatively well-calibrated satellite records. The satellite observations show similar changes in FR and SCE durations, with contrasting decreasing and increasing seasonal trends between spring/summer and fall/winter conditions, respectively. We find generally strong correspondence between mean annual and seasonal FR and SCE duration changes, but with regional variations in these relationships for different climate zones and snow cover regimes, and generally closer coupling at higher latitudes where the FR and SCE seasons are a larger portion of the annual cycle. The geographic extent of FR conditions is generally larger than SCE in fall and winter, resulting in large areas of freezing conditions without an insulating snow layer. In contrast, FR area is smaller than SCE in the spring, while regional

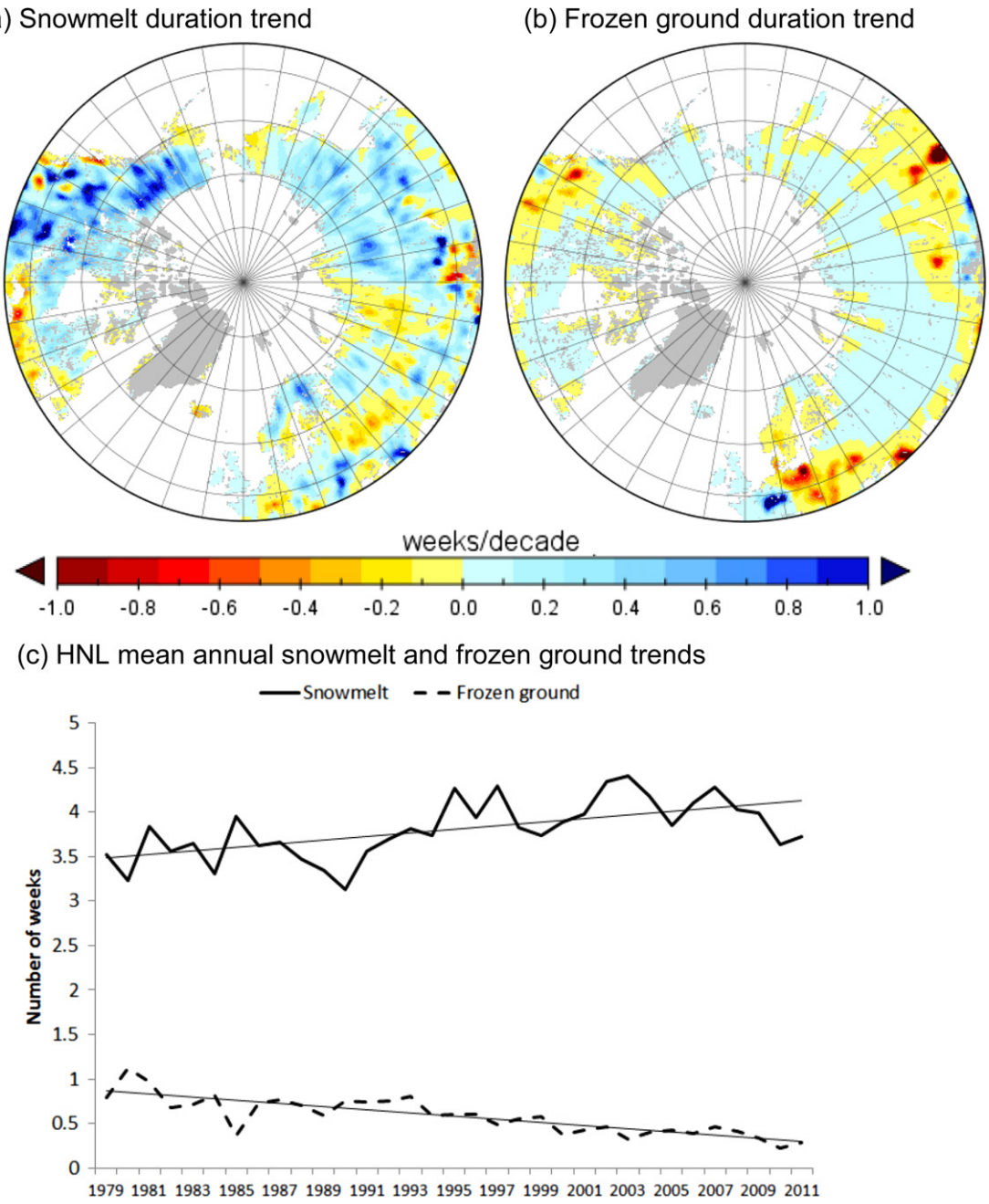

Figure 5. Regional Kendall's tau trend patterns (weeks decade^{-1}) of (a) snowmelt, (b) frozen ground durations, and (c) annual variation and significant trends ($p < 0.01$) of HNL mean snowmelt and frozen ground durations for the 1979–2011 record; mapped areas outside the HNL study domain are denoted in grey (land) and white (100% open water), while spatial convolution of a Gaussian weighting filter was also applied to the maps.

differences in these two parameters delineate the zone and duration of snowmelt. Our results document an increasing HNL trend in the snowmelt duration, which predominantly occurs from an extension of snow cover and transitional FT conditions in the fall, and is coincident with regional warming. We also find a significant HNL decreasing trend in FR ground duration year-round, but which largely occurs over the southern HNL domain rather than the northern boreal-arctic permafrost zone.

The timing and duration of FR ground in the absence of an insulating snowpack can influence the soil thermal regime and ecosystem processes, including soil litter decomposition and respiration, and potential freezing injury to plants (Beier *et al* 2008, Saito *et al* 2013). Our results show a general decreasing trend in FR ground duration over the HNL domain coincident with regional warming trends and consistent with a general relaxation of FR season constraints to land surface water mobility and ecosystem processes (Kim *et al* 2014a). However, the effect of these changes on regional soil temperature trends is uncertain because the soil thermal regime is strongly coupled to changes in timing and duration of SCE,

which shows a more variable response pattern, as well as changes in snow depth and structure from which we have a general lack of regional information.

Significant snowmelt duration increases occur over 24.3% of the domain characterized by underlying permafrost. These changes may have considerable impacts on the terrestrial energy budget and land-atmosphere climate feedbacks associated with lower surface albedos and enhanced net solar radiation loading under wet snowpack conditions (Zhang *et al* 2003), and associated non-FR season increases in surface latent energy exchange and evaporation (Zhang *et al* 2011). An extended snowmelt trend may also promote warmer soil temperatures, deepening active layer development and permafrost warming (Zhang *et al* 2005, Anisimov 2007). Snow structural changes from increasing melt events may also promote the development of thick ice layers, adversely affecting animal habitats, migration and foraging success (Bartsch *et al* 2010, Vincent *et al* 2011). Further research is needed to clarify the impacts of these changes on HNL ecosystems and regional climate feedbacks. Continuity of the FT-ESDR and SCE records enabled from ongoing satellite observations will support future studies of continuing changes and longer-term trends in these parameters.

References

Aanderud Z T, Jones S E, Schoolmaster D R Jr, Fierer N and Lennon J T 2013 Sensitivity of soil respiration and microbial communities to altered snowfall *Soil Biol. Biochem.* **57** 217–27

Anisimov O A 2007 Potential feedback of thawing permafrost to the global climate system through methane emission *Environ. Res. Lett.* **2** 045016

Barichivich J, Briffa K R, Mynani R, van der Schrier G, Dorigo W, Tucker C J, Osborn T J and Melvin T M 2014 Temperature and snow-mediated moisture controls of summer photosynthetic activity in northern terrestrial ecosystems between 1982 and 2011 *Remote Sens.* **2014** 1390–431

Bartsch A, Kumpula T, Forbes B C and Stammler F 2010 Detection of snow surface thawing and refreezing in the Eurasian Arctic with QuickSCAT: implications for reindeer herding *Ecol. Appl.* **20** 234–2358

Beier C M, Sink S E, Hennon P E, D'Amore D V and Juday G P 2008 Twentieth-century warming and the dendroclimatology of declining yellow-cedar forests in southeastern Alaska *Can. J. Forest Res.* **38** 1319–34

Betts A K, Desjardins R, Worth D, Wang S and Li J 2014 Coupling of winter climate transitions to snow and clouds over the Prairies *J. Geophys. Res. Atmos.* **119** 1118–39

Bewley D, Essery R, Pomeroy J and Menard C 2010 Measurements and modelling of snowmelt and turbulent heat fluxes over shrub tundra *Hydrol. Earth Syst. Sci.* **14** 1331–40

Brodzik M and Armstrong R 2013 *Northern Hemisphere EASE-Grid 2.0 Weekly Snow Cover and Sea Ice Extent. Version 4. (1979–2011)* (Boulder, CO: NASA DAAC at the National Snow and Ice Data Center) (http://nsidc.org/data/docs/daac/nsidc0046_nh_ease_snow_seaice.gd.html)

Brodzik M J, Billingsley B, Haran T, Raup B and Savoie M H 2012 EASE-grid 2.0: incremental but significant improvements for Earth-gridded data sets *ISPRS Int. J. Geo-Inf.* **1** 32–45

Brodzik M J and Knowles K W 2002 EASE-grid: a versatile set of equal-area projections and grids *Discrete Global Grids* ed M Goodchild (Santa Barbara, CA: National Center for Geographic Information and Analysis)

Brown J, Ferrians O, Heginbottom J A and Melnikov. E 2014 *Circum-Arctic Map of Permafrost and Ground-Ice Conditions* (Boulder, CO: National Snow and Ice Data Center) (http://nsidc.org/data/ggd318)

Brown R D and Derksen C 2013 Is Eurasian October snow cover extent increasing? *Environ. Res. Lett.* **8** 024006

Brown R D and Robinson D A 2011 Northern Hemisphere spring snow cover variability and change over 1922–2010 including an assessment of uncertainty *The Cryosphere* **5** 219–29

Brown R, Derksen C and Wang L 2007 Assessment of spring snow cover duration variability over northern Canada from satellite datasets *Remote Sens. Environ.* **111** 367–81

Bulygina O N, Razuvaev V N and Korshunova N N 2009 Changes in snow cover over Northern Eurasia in the last few decades *Environ. Res. Lett.* **4** 045026

Callaghan T V *et al* 2011 The changing face of arctic snow cover: a synthesis of observed and projected changes *AMBIO* **40** 17–31

Chapin F S III *et al* 2005 Role of land-surface changes in arctic summer warming *Science* **310** 657–60

Cohen J L, Furtado J C, Barlow M, Alexeev V A and Cherry J E 2012a Assymmetric seasonal temperature trends *Geophys. Res. Lett.* **39** L04705

Cohen J L, Furtado J C, Barlow M A, Alexeev V A and Cherry J E 2012b Arctic warming, increasing snow cover and widespread boreal winter cooling *Environ. Res. Lett.* **7** 014007

Daly C, Halbleib M, Smith J I, Gibson W P, Doggett M K, Taylor G H, Curtis J and Pasteris P P 2008 Physiographically sensitive mapping of climatological temperature and precipitation across the conterminous United States *Int. J. Climatol.* **28** 2031–64

Daniels L D, Maertens T B, Stan A B, Mccloskey S P J, Cochrane J D and Gray R W 2011 Direct and indirect impacts of climate change on forests: three case studies from British Columbia *Can. J. Plant Pathology* **33** 108–16

Dee D P *et al* 2011 The ERA-Interim reanalysis: configuration and performance of the data assimilation system *Q. J. R. Meteorol. Soc.* **137** 553–97

Derksen C and Brown R 2012 Spring snow cover extent reductions in the 2008–2012 period exceeding climate model projectios *Geophys. Res. Lett.* **39** L19504

Dery S J and Brown R D 2007 Recent Northern Hemisphere snow cover extent trends and implications for the snow-albedo feedback *Geophys. Res. Lett.* **34** L22504

Du J, Kimball J S, Azarderakhsh M, Dunbar R S, Moghaddam M and McDonald K C 2014 Classification of Alaska spring thaw characteristics using L-band Radar remote sensing *IEEE Trans. Geosci. Remote Sens.* **53** 542–56

Du E, Zhou Z, Li P, Jiang L, Hu X and Fang J 2013 Winter soil respiration during soil-freezing process in a boreal forest in Northeast China *J. Plant Ecol.* **6** 349–57

Dye D G 2002 Variability and trends in the annual snow-cover cycle in Northern Hemisphere land areas, 1979–2000 *Hydrol. Process.* **16** 3065–77

Estilow T and Robinson D & National Center for Atmospheric Research Staff (ed)2013 *The Climate Data Guide: Snow Cover Extent (Northern Hemisphere) Climate Data Record* (last modified 28 Aug 2013) (https://climatedataguide.ucar.edu/climate-data/snow-cover-extent-northern-hemisphere-climate-data-record-rutgers)

Euskirchen E S, McGuire A D and Chapin F S III 2007 Energy feedbacks of northern high-latitude ecosystems to the climate change system due to reduced snow cover during 20th century warming *Glob. Clim. Biol.* **13** 2425–38

Frei A, Tedesco M, Lee S, Foster J, Hall D K, Kelly R and Robinson D A 2012 A review of global satellite-derived snow products *Adv. Space Res.* **50** 1007–29

Haei M, Oquist M G, Kreyling J, Ilstedt U and Laudon H 2013 Winter climate controls soil carbon dynamics during summer in boreal forests *Environ. Res. Lett.* **8** 042017

Helfrich S R, McNamara D, Ramsay B H, Baldwin T and Kasheta T 2007 Enhancements to, and forthcoming developments in

the interactive multisensor snow and ice mapping system (IMS) *Hydrol. Process.* **21** 1576–86
Jeganathan C, Dash J and Atkinson P M 2014 Remotely sensed trends in the phenology of northern high latitude terrestrial vegetation, controlling for land cover change and vegetation type *Remote Sens. Environ.* **143** 154–70
Kim Y, Kimball J S, Zhang K, Didan K, Velicogna I and McDonald K C 2014a Attribution of divergent northern vegetation growth responses to lengthening non-frozen seasons using satellite optical-NIR and microwave remote sensing *Int. J. Remote Sens.* **35** 3700–21
Kim Y, Kimball J S, Glassy J and McDonald K C 2014b *MEaSUREs Global Record of Daily Landscape Freeze/Thaw Status. Version 3. (1979–2011)* (Boulder, CO: NASA DAAC at the National Snow and Ice Data Center) (doi:10.5067/MEASURES/CRYOSPHERE/nsidc-0477.003)
Kim Y, Kimball J S, Didan K and Henebry G M 2014c Responses of vegetation growth and productivity to spring climate indicators in the conterminous Unites States derived from satellite remote sensing data fusion *Agric. Forest Meteorol.* **194** 132–43
Kim Y, Kimball J S, Zhang K and McDonald K C 2012 Satellite detection of increasing northern hemisphere non-frozen seasons from 1979 to 2008: implications for regional vegetation growth *Remote Sens. Environ.* **121** 472–87
Kim Y, Kimball J S, McDonald K C and Glassy J 2011 Developing a global data record of daily landscape freeze/thaw status using satellite passive microwave remote sensing *IEEE Trans. Geosci. Remote Sens.* **49** 949–60
Kimball J S, McDonald K C, Keyser A R, Frolking S and Running S W 2001 Application of the NASA scatterometer (NSCAT) for determining the daily frozen and non-frozen landscape of Alaska *Remote Sens. Environ.* **75** 113–26
Kreyling J, Haei M and Laudon H 2012 Absence of snow cover reduces understory plant cover and alters plant community composition in boreal forests *Oecologia* **168** 577–87
Ling F and Zhang T 2003 Impact of the timing and duration of seasonal snow cover on the active layer and permafrost in the Alaskan Arctic *Permafrost Periglacial Process.* **14** 141–50
Marsh P, Bartlett P, MacKay M, Pohl S and Lantz T 2010 Snowmelt energetics at a shrub tundra site in the western Canadian Arctic *Hydrol. Process.* **24** 3603–20
Mioduszewski J R, Rennermalm A K, Robinson D A and Mote T L 2014 Attribution of snowmelt onset in Northern Canada *J. Geophys. Res.: Atmos.* **119** 9638–53
Mortin L, Schroder T M, Hansen A W, Holt B and McDonald K C 2012 Mapping of seasonal freeze/thaw transitions across the pan-Arctic land and sea ice domains with satellite radar *J. Geophys. Res.* **117** C08004
Mudryk L R, Kushner P J and Derksen C 2014 Interpreting observed northern hemisphere snow trends with large ensembles of climate simulations *Clim. Dyn.* **43** 345–59
Nolin A W 2010 Recent advances in remote sensing of seasonal snow *J. Glaciol.* **56** 1141–50
Painter T H, Rittger K, McKenzie C, Slaughter P, Davis R E and Dozier J 2009 Retrieval of subpixel snow covered area, grain size, and albedo from MODIS *Remote Sens. Environ.* **113** 868–79
Park H, Fedorov A N, Zheleznyak M N, Konstantinov P Y and Walsh J E 2014 Effect of snow cover on pan-Arctic permafrost thermal regimes *Clim. Dyn.* **44** 2873–95
Peel M C, Finlayson B L and McMahon T A 2007 Updated world map of the Köppen–Geiger climate classification *Hydrol. Earth Syst. Sci.* **11** 1633–44
Pomeroy J W, Bewley D S, Essery R L H, Hedstrom N R, Link T, Granger R J, Sicart J E, Ellis C R and Janowicz J R 2006 Shrub tundra snowmelt *Hydrol. Process.* **20** 923–41
Robinson D and Frei A 2000 Seasonal variability of northern hemisphere snow extent using visible satellite data *Prof. Geogr.* **52** 307–15
Saito K, Zhang T, Yang D, Marchenko S, Barry R G, Romanovsky V and Hinzman L 2013 Influence of the physical terrestrial Arctic in the eco-climate system *Ecol. Appl.* **23** 1778–97
Semmens K A, Ramage J, Bartsch A and Liston G E 2013 Early snowmelt events: detection, distribution, and significance in a major sub-arctic watershed *Environ. Res. Lett.* **8** 014020
Sturm M, Douglas T, Racine C and Liston G E 2005 Changing snow and shrub conditions affect albedo with global implications *J. Geophys. Res.* **110** G01004
Sturm M, Holmgren J and Liston G E 1995 A seasonal snow cover classification system for local to global applications *J. Clim.* **8** 1261–83
Tang Z, Wang J, Li H and Yan L 2013 Spatialtemporal changes of snow cover over the Tibetan plateau based on cloud-removed moderate resolution imaging spectroradiometer fractional snow cover product from 2001 to 2011 *J. Appl. Remote Sens.* **7** 073582
Vincent W F, Callaghan T V, Dahl-Jensen D, Johansson M, Kovacs K M, Michel C, Prowse T, Reist J D and Sharp. M 2011 Ecological implications of changes in the Arctic cryosphere *AMBIO* **40** 87–99
Wang X and Zender C S 2011 Arctic and antarctic diurnal and seasonal variations of snow albedo from multiyear baseline surface radiation network measurements *J. Geophys. Res.* **116** F03008
Yue S and Pilon P 2004 A comparison of the power of the t test, Mann−Kendall and bootstrap tests for trend detection *Hydrol. Sci. J.* **49** 21–37
Zhang K, Kimball J S, Kim Y and McDonald K C 2011 Changing freeze-thaw seasons in northern high latitudes and associated influences on evapotranspiration *Hydrol. Process.* **25** 4142–51
Zhang K, Kimball J S, McDonald K C, Cassano J J and Running S W 2007 Impacts of large-scale oscillations on pan-Arctic terrestrial net primary production *Geophys. Res. Lett.* **34** L21403
Zhang T *et al* 2005 Spatial and temporal variability in active layer thickness over Russian Arctic drainage basin *J. Geophys. Res.* **110** D16101
Zhang T, Scambos T, Haran T, Hinzman L D and Kane D L 2003 Ground-based and satellite-derived measurements of surface albedo on the north slope of Alaska *J. Hydrometeorol.* **4** 77–91